Fermi National Accelerator Laboratory

Effect of Finite Nucleon Mass on Primordial Nucleosynthesis

Robert E. Lopez, Michael S. Turner and Geza Gyuk

Fermi National Accelerator Laboratory
P.O. Box 500, Batavia, Illinois 60510

February 1998

Disclaimer

Distribution

EFFECT OF FINITE NUCLEON MASS ON PRIMORDIAL NUCLEOSYNTHESIS

Robert E. Lopez,[1] Michael S. Turner,[1,2,3] and Geza Gyuk[4]

[1]*Department of Physics,*
The University of Chicago, Chicago, IL 60637-1433
[2]*NASA/Fermilab Astrophysics Center,*
Fermi National Accelerator Laboratory, Batavia, IL 60510-0500
[3]*Department of Astronomy & Astrophysics,*
Enrico Fermi Institute, The University of Chicago, Chicago, IL 60637-1433
[4]*International School for Advanced Studies (SISSA)*
Via Beirut 4, 34014 Trieste, Italy

ABSTRACT

By numerically evaluating five-dimensional phase-space integrals, we have calculated the small effect of finite nucleon mass on the weak-interaction rates that interconvert protons and neutrons in the early Universe. We have modified the standard code for primordial nucleosynthesis to include these corrections and find a small, systematic increase in the ^{4}He yield, $\Delta Y/Y \simeq (0.47-0.50)\%$, depending slightly on the value of the baryon-to-photon ratio η. The fractional changes in the abundances of D, ^{3}He, and ^{7}Li range from 0.06% to 2.8% for $10^{-11} \leq \eta \leq 10^{-8}$.

1 Introduction

Primordial nucleosynthesis is one of the cornerstones of the hot big-bang cosmology. The consistency between its predictions for the abundances of D, ^{3}He, ^{4}He and ^{7}Li and their inferred primordial abundances provides its earliest test. Further, big-bang nucleosynthesis has been used to obtain the best determination of the baryon density [1, 2, 3] and to test particle-physics theories, e.g., the stringent limit to the number of light neutrino species [4, 5, 6].

Scrutiny of primordial nucleosynthesis, both on the theoretical side and on the observational side, has been constant: Reaction rates have been updated and their uncertainties quantified [7, 8, 9]; finite-temperature corrections have been taken into account [10]; the effect of inhomogeneities in the baryon density explored [11]; the slight effect of the heating of neutrinos by $e^\pm$ annihilations has been computed [12, 13]; the primordial abundance of ^{7}Li has been put on a firm basis and its destruction in stars has been studied [14, 15, 16, 17, 18, 19, 20, 21]; the production and destruction of ^{3}He and the destruction of D have been studied [2, 22, 23, 24]; and astrophysicists now argue about the third significant figure in the primordial ^{4}He abundance [25, 26, 27].

A measure of the progress in this endeavour is provided by the shrinking of the "concordance region" of parameter space. The predicted and measured primordial abundances agree provided: the baryon-to-photon ratio lies in the narrow interval $2 \times 10^{-10} \leq \eta \leq 7 \times 10^{-10}$ and the equivalent number of light neutrino species $N_\nu \leq 4$ [1, 3]. The shrinking of the concordance interval motivates the study of smaller and smaller effects. In particular, once the primeval deuterium abundance is accurately determined in high-redshift hydrogen clouds, the baryon-to-photon ratio will be pegged to an accuracy of order 10%, and recent progress suggests that this will happen sooner rather than later [28]. In turn, this will reduce the uncertainty in the predicted ^{4}He abundance due to the baryon density to $\Delta Y \simeq \pm 0.005$.

The weak-interaction rates govern the neutron-to-proton ratio and thereby are crucial to the outcome of nucleosynthesis; e.g., the mass fraction of ^{4}He produced is roughly twice the neutron fraction at the time nucleosynthesis commences ($T \sim 0.08\,\mathrm{MeV}$). In the standard code [29, 30] these rates are computed in the infinite-nucleon-mass limit because this simplifies the expressions for the rates to one-dimensional integrals. The finite-mass corrections involve terms of order m_e/m_N, T/m_N, and Q/m_N, which are all of the order of 0.1%. Here m_e is the electron mass, m_N is the nucleon mass, $T \sim \mathcal{O}(\mathrm{MeV})$ is the temperature during the epoch of nucleosynthesis, and $Q = m_n - m_p = 1.293\,\mathrm{MeV}$ is the neutron-proton mass difference. As it turns out, the corrections to the rates are actually of order a few percent, so that the change in ^{4}He abundance is expected to be a few parts in the third significant figure ($\Delta Y/Y \sim -0.5\delta\,\mathrm{rate/rate}$).

Because the third significant figure of the primordial ^{4}He abundance is now relevant, we set out to calculate the finite-nucleon-mass corrections to the weak-interaction rates by numerically integrating the exact expressions for the rates. This involved accurately ($\lesssim 0.1\,\%$) evaluating five-dimensional rate integrals. We incorporated our results into the
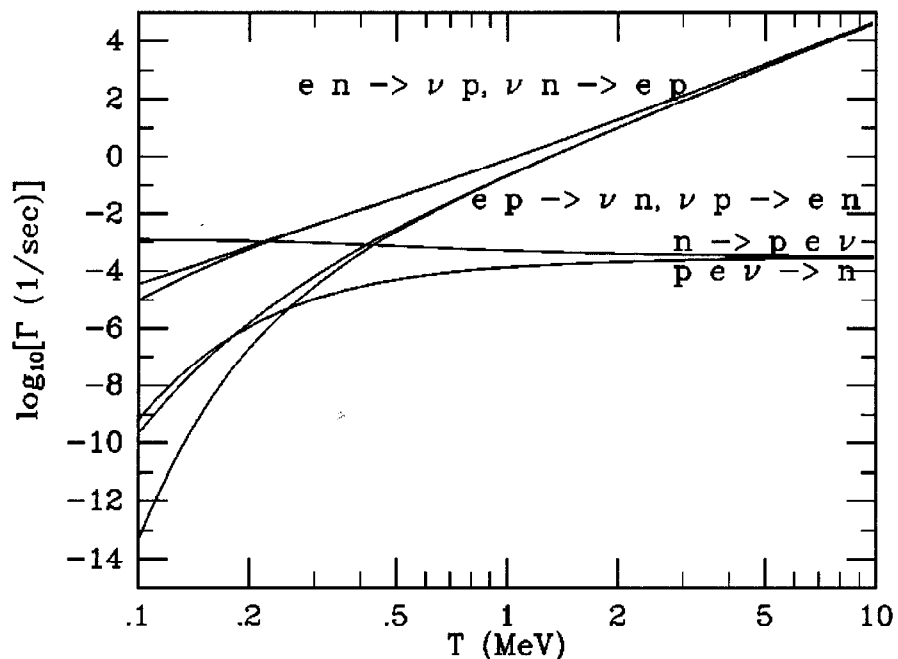
Figure 1: Weak rates as a function of temperature (infinite-nucleon-mass limit). Note, freeze-out of the n/p ratio occurs at $T \simeq 0.8\,\mathrm{MeV}$ and nucleosynthesis begins in earnest at $T \simeq 0.1\,\mathrm{MeV}$.

standard nucleosynthesis code and found that $\Delta Y/Y \approx (0.47 - 0.50)\%$, depending on the value of η. In the next Section we discuss the weak rates, and in the following Section finite-mass corrections to the weak rates. In Sec. IV we discuss our changes to the standard nucleosynthesis code, and we finish with a discussion of our results for the changes in the yields of ^{4}He and the other light elements.

2   Weak-interaction Rates

The weak interactions that interconvert neutrons and protons, $n \leftrightarrow p + e + \nu$, $n + e \leftrightarrow p + \nu$, and $n + \nu \leftrightarrow p + e$, play a crucial role as they govern the neutron fraction, and the neutron fraction ultimately determines the amount of nucleosynthesis that takes place. (Here and throughout we use e to indicate electron or positron, and ν to indicate electron neutrino or antineutrino; the appropriate particle or antiparticle designation follows from charge and lepton-number conservation.) For reference, Fig. 1 shows the weak rates as a function of temperature.

2

2.1 Rate Expressions

Generally, the weak-interaction rates may be expressed as integrals over phase space. For definiteness, consider the process $ep \to \nu n$. The other processes involve similar expressions. The rate, reactions per incident nucleon per time, is given by a twelve-dimensional integral,

$$\Gamma_{ep\leftrightarrow\nu n} = \frac{1}{n_p} \int \prod_i d\Pi_i (2\pi)^4 \left|\mathcal{M}\right|^2 \delta^{(4)}(e + p - \nu - n) f_e f_p (1 - f_\nu)(1 - f_n), \tag{1}$$

where n_p is the number density of the incident nucleon, $d\Pi_i = d^3 p_i / [(2\pi)^3 2 E_i]$ is the Lorentz invariant phase-space element, $\left|\mathcal{M}\right|^2$ is the weak-interaction matrix element summed over initial and final spins (see Appendix A), e, p, ν and n are the four-momenta of the particles, and the delta function $\delta^{(4)}(e + p - \nu - n)$ expresses conservation of four-momentum. In the rest frame of the thermal radiation, the phase-space densities f_e, f_p, f_ν and f_n are given by the usual Fermi-Dirac distribution functions.

Assuming only the isotropy of space, we can integrate over $d\Omega_e$, the direction of the electron's three-momentum and $d\phi_p$, the azimuthal angle of the proton's three-momentum. After applying conservation of three-momentum to eliminate $d^3 p_n$ and conservation of energy to eliminate dp_ν, the expression simplifies to the following five-dimensional integral:

$$\Gamma_{ep\leftrightarrow\nu n} = \frac{1}{2^9 \pi^6 n_p} \int dp_e dp_p d\cos\theta_p d\cos\theta_\nu d\phi_\nu$$

$$\times \frac{p_e^2 p_p^2 E_\nu}{E_e E_p E_n} \frac{1}{\mathcal{J}} \left|\mathcal{M}\right|^2 f_e f_p (1 - f_\nu)(1 - f_n), \tag{2}$$

$$\mathcal{J} = 1 + \frac{E_\nu}{E_n} \left(1 - \frac{(\mathbf{p}_e + \mathbf{p}_p) \cdot \mathbf{p}_\nu}{E_\nu^2}\right), \tag{3}$$

where E_e, E_p, E_ν, and E_n denote the energies of the respective particles and $\mathcal{J}$ is the Jacobian introduced in integrating the energy part of the delta function. We take $\mathbf{p}_e$ parallel to the polar axis ($\theta_e = \phi_e = 0$) and $\phi_p = 0$. We need an expression for E_ν in terms of the integration variables $p_e, p_p, \theta_p, \theta_\nu$, and ϕ_ν; it is given by

$$p_\nu = \frac{A^2 B + 2E\sqrt{A^4 - m_\nu^2(4E^2 - B^2)}}{4E^2 - B^2},$$

$$A^2 \equiv 2E_e E_p + m_\nu^2 - m_n^2 - m_e^2 - m_p^2 - 2 p_e p_p \cos\theta_p,$$

$$B \equiv 2\left[p_e \cos\theta_\nu + p_p \left(\cos\theta_p \cos\theta_\nu + \sin\theta_p \sin\theta_\nu \cos\phi_\nu\right)\right]. \tag{4}$$

where $E = E_e + E_p$. If m_ν is taken to be zero (or very small) these equations simplify further. We left them in this form because for two-body processes in which the electron is the outgoing lepton, $m_\nu \to m_e \neq 0$.

3

2.2 Infinite-Mass Approximation

If the nucleons are assumed to be infinitely massive,[1] two things happen. The kinematics simplifies because the kinetic energy of the nucleons can be neglected ($E_e - E_\nu = Q$), and the matrix element simplifies, $|\mathcal{M}|^2 = 2G_F^2(1 + 3g_A^2)2E_e2E_p2E_\nu2E_n$. Here $G_F = 1.166 \times 10^{-5}\,\mathrm{GeV}^{-2}$ is the Fermi constant and $g_A \simeq 1.257$ is the ratio of axial to vector coupling to the nucleon. The rate expression now reduces to the familiar form [31]:

$$\Gamma^\infty_{ep \leftrightarrow \nu n} = \frac{G_F^2(1 + 3g_A^2)m_e^5}{2\pi^3} \int_q^\infty \frac{\epsilon(\epsilon^2 - q^2)^{1/2}}{[1 + \exp(\epsilon z)]\,[1 + \exp((q - e)z_\nu)]}, \tag{5}$$

where T is the photon temperature, T_ν is the neutrino temperature, $\epsilon \equiv E_e/m_e$, $z \equiv m_e/T$, and $z_\nu \equiv m_e/T_\nu$. Expressions for the other five $n \leftrightarrow p$ processes are similar. This is the approximation used in the standard nucleosynthesis code.

In the era preceding nucleosynthesis, when to a good approximation baryons exist as free neutrons and protons, the neutron fraction X_n is governed by

$$\dot{X}_n = -X_n\Gamma_{n \to p} + (1 - X_n)\Gamma_{p \to n}, \tag{6}$$

where $X_p = 1 - X_n$, and

$$\begin{aligned}
\Gamma_{p \to n} &\equiv \Gamma_{ep \to \nu n} + \Gamma_{\nu p \to en} + \Gamma_{pe\nu \to n} \\
\Gamma_{n \to p} &\equiv \Gamma_{en \to \nu p} + \Gamma_{\nu n \to ep} + \Gamma_{n \to pe\nu}.
\end{aligned} \tag{7}$$

In thermal equilibrium, which holds when the rates are much greater than the expansion rate of the Universe,

$$\left(\frac{n}{p}\right) = \frac{\Gamma_{p \to n}}{\Gamma_{n \to p}} = \left(\frac{m_n}{m_p}\right)^{3/2} e^{-Q/T}. \tag{8}$$

In the infinite-mass limit, $m_n/m_p = 1$, and

$$\left(\frac{n}{p}\right)^\infty = \frac{\Gamma^\infty_{p \to n}}{\Gamma^\infty_{n \to p}} = e^{-Q/T}. \tag{9}$$

The second equality in both equations is just detailed balance, which is one of the checks that we will use to test our results.

3   Finite-Mass Corrections

We carried out the five-dimensional integration using the Monte Carlo technique. The challenge was to compute a finite-mass correction, whose size is of order a few percent, to a relative accuracy of a few percent. Hence, we had to evaluate the rate integral to order

---

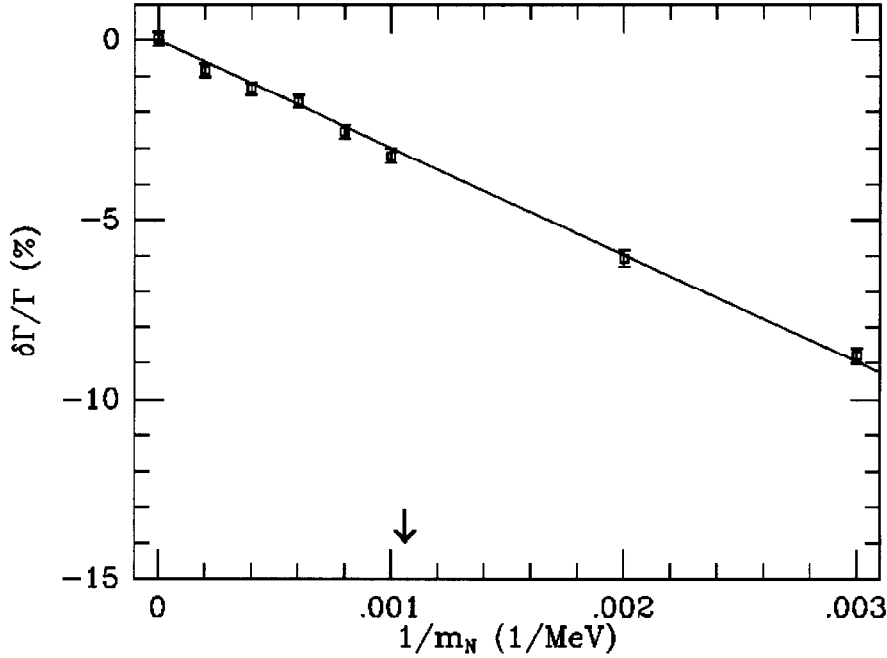[1]More precisely, $m_n, m_p \to \infty$ with $m_n - m_p = Q$ fixed.

Figure 2: Finite-nucleon-mass correction to $\nu p \to en$ at $T = 1.0\,\mathrm{MeV}$ as a function of $1/m_N$. The error bars represent the estimated statistical uncertainty. The arrow indicates the actual value of the nucleon mass, $m_N \simeq 940$ MeV. Note, the correction vanishes for $m_N \to \infty$ and is linear in $1/m_N$.

0.1% accuracy. The statistical uncertainty in integrating the rate expressions was typically around 0.3% for several minutes of computer time. Since this scales as $1/\sqrt{N}$, where N is the number of function evaluations, we could have achieved the accuracy requirements by simply increasing the integration time by a factor of ten or so. However, we found a more efficient way of proceeding, which also allowed other checks to be made.

For $E/m_N \ll 1$ the finite-mass correction to the weak rates should vary linearly with $1/m_N$ ($E \sim 1\,\mathrm{MeV}$ is the characteristic energy scale: $E \sim Q, m_e, T$.) As $E/m_N \to 0$, the correction must approach zero. We adopted the following strategy. We performed a series of runs where we fixed the temperature but varied the nucleon mass. We found the finite-mass correction ($\equiv \delta\Gamma = \Gamma - \Gamma^\infty$) by applying a linear fit to the data and interpolating to $m_N \simeq 940$ MeV. Figure 2 shows the result of this procedure for the process $ep \to \nu n$. The linearity of $\delta\Gamma/\Gamma$ in $1/m_N$ is manifest as is the intercept at $\delta\Gamma/\Gamma = 0$ for $m_N \to \infty$.

We found that the finite-mass correction for each process varies linearly with temperature. Therefore, we applied a linear fit to the correction as a function of temperature. In the end we were able to achieve the required order 0.1% absolute accuracy in the rate integrals. Figure 3 shows the finite-mass corrections $\delta\Gamma/\Gamma$ for all six processes that interconvert neutrons and
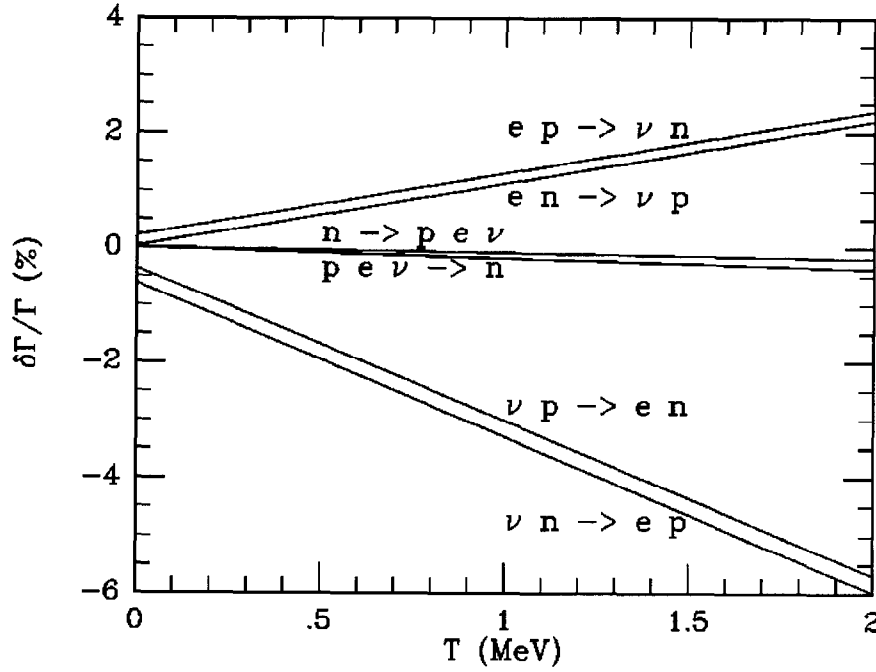
5

Figure 3: Finite-nucleon-mass corrections to the weak rates as a function of temperature.

protons. The corrections are, as expected, of order a few percent.

3.1   Tests of finite-mass corrections

We applied several checks to our results. The simplest was to let $1/m_N$ vary. As $1/m_N \to 0$ the finite-mass rate corrections should approach zero; Fig. 2 illustrates that they do. While Fig. 2 illustrates convergence for a particular process and temperature, convergence was observed for all processes and temperatures.

Another test is provided by detailed balance. Detailed balance requires that

$$\left(\frac{\Gamma_{p \to n}}{\Gamma_{n \to p}}\right) = \left(\frac{n}{p}\right)_{\rm EQ} = \left(\frac{m_n}{m_p}\right)^{3/2} e^{-Q/T} \simeq \left(\frac{3}{2}\frac{Q}{m_N} + 1\right) e^{-Q/T}, \tag{10}$$

while the neutrinos are coupled to the photon plasma and $T_\nu = T_\gamma$. We numerically determined $\Gamma_{n \to p}/\Gamma_{p \to n}$, and expressed it as

$$\frac{\Gamma_{p \to n}}{\Gamma_{n \to p}} \simeq \left(\frac{3}{2}\frac{Q}{m_N}\alpha + 1\right) e^{-Q/T}; \tag{11}$$

$\alpha = 1$ corresponds to detailed balance being satisfied. Figure 4 shows that detailed balance is satisfied while the neutrinos are coupled to the photons and also when the neutrino temperature is set equal to the photon temperature.
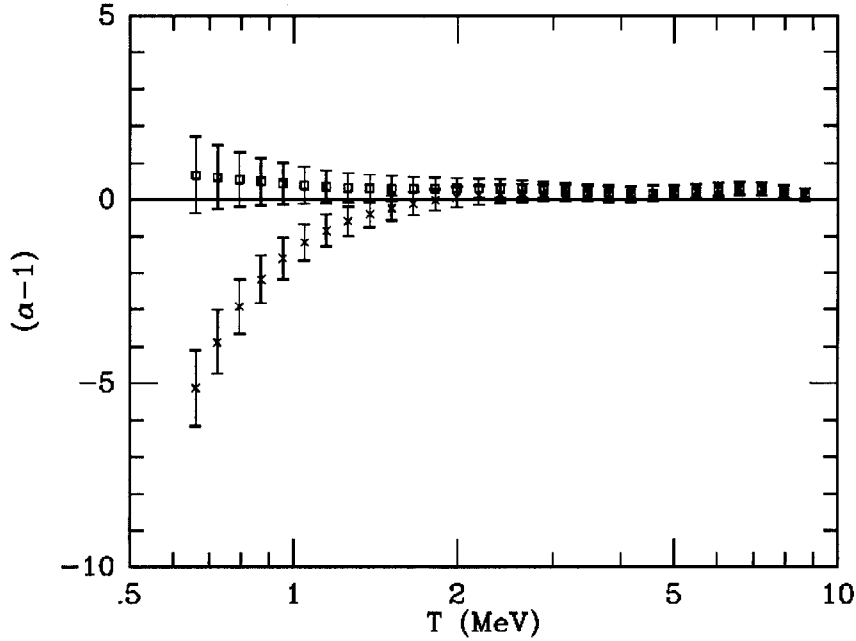
6

Figure 4: Detailed-balance test. For $\alpha = 1$ detailed balance is satisfied (see text). For the boxes, $T_\nu = T_\gamma$ is enforced; for the crosses neutrinos are assumed to be decoupled, so that $T_\nu < T_\gamma$ for $T_\gamma \lesssim 1\text{MeV}$. Since the finite-mass corrections are obtained from fits to $1/m_N$ and T_γ, the errors are strongly correlated.

Finally, we were able to derive an independent and simpler expression for the finite-mass rates but using the infinite-mass matrix element. This provides a check of the complicated kinematics that arise for $m_N \neq \infty$. In Eq. (1) the three-momentum part of the delta function is expanded in complex exponentials,

$$\Gamma_{ep\to\nu n} = \frac{1}{n_p} \int \prod_i d\Pi_i d^3x (2\pi) e^{i\mathbf{x}\cdot(\mathbf{p}_e + \mathbf{p}_p - \mathbf{p}_\nu - \mathbf{p}_n)} |\mathcal{M}|^2$$
$$\times \delta(E_e + E_p - E_\nu - E_n) f_e f_p (1 - f_\nu)(1 - f_n). \tag{12}$$

If the integrand has no angular dependence, as is the case for the infinite-mass matrix element, the expression can be reduced to three-dimensional integral. (With angular dependence, the reduction can be done term by term in the angular expansion of the matrix element, but the resulting expression becomes very complicated.) For the infinite-mass matrix element all of the angular integrals can be done,

$$\Gamma^3_{ep\to\nu n} = \frac{G_F^2 (1 + 3g_A^2)}{\pi^6 n_p} \int \prod_i dp_i \; p_i \sin(xp_i) \frac{d^3x}{x^2}$$
$$\times \delta(E_e + E_p - E_\nu - E_n) f_e f_p (1 - f_\nu)(1 - f_n). \tag{13}$$

7

The integral over dx can be done by a standard contour integration,

$$\Gamma^3_{ep \to \nu n} = -\frac{G_F^2(1+3g_A^2)}{2^4\pi^5 n_p} \int dE_e dE_p dE_\nu E_e E_p E_\nu (E_p + E_e - E_\nu)$$

$$\times (\sum_{i=1}^{8} t_i) f_e f_p (1 - f_\nu)(1 - f_n), \tag{14}$$

where the energy delta function has been used to carry out the dE_n integral and

$$\sum_{i=1}^{8} t_i = |p_e + p_p + p_\nu + p_n| + |p_e + p_p - p_\nu - p_n|$$

$$+ |p_e - p_p + p_\nu - p_n| + |p_e - p_p - p_\nu + p_n|$$

$$- |p_e + p_p + p_\nu - p_n| - |p_e + p_p - p_\nu + p_n|$$

$$- |p_e - p_p + p_\nu + p_n| - |p_e - p_p - p_\nu - p_n|. \tag{15}$$

Using standard techniques we carried out the numerical integration.

For our test we compare Γ^3 with the rate obtained by inserting the infinite-mass matrix element into Eq. (2). This rate, denoted by Γ^5, is given by

$$\Gamma^5_{ep \to \nu n} = \frac{G_F^2(1+3g_A^2)}{2^4\pi^6 n_p} \int dp_e dp_p d\cos\theta_p d\cos\theta_\nu d\phi_\nu$$

$$\times p_e^2 p_p^2 p_\nu E_\nu \frac{1}{\mathcal{J}} f_e f_p (1 - f_\nu)(1 - f_n). \tag{16}$$

Formally, Γ^3 and Γ^5 are identical. Numerically, they are computed using independent techniques. Comparing them provides a stringent test of kinematics. Figure 5 shows this comparison as a function of m_N with $T = 5$ MeV. Figure 6 shows the comparison as a function of T with $m_N = 100$ MeV. In both cases, Γ^3 and Γ^5 agree within estimated numerical uncertainties. In conclusion, because our finite-mass rate corrections pass these three important tests, we have confidence that they are correct and accurate.

4   Changes to the Standard Code

The standard code calculates the weak rates at each temperature step. (The user is offered the choice of either integrating the rates of using fits to them. We chose to have the code integrate the rates at each step.) The rates are obtained by integrating equations like Eq. (5), which assume that the nucleons are infinitely massive. Our approach was to implement the finite-mass rate corrections as a multiplicative factor at each temperature step:

$$\Gamma_{p \to n} = \Gamma^\infty_{p \to n} \left(1 + \frac{\delta\Gamma}{\Gamma}\right)$$

$$\Gamma_{n \to p} = \Gamma^\infty_{n \to p} \left(1 + \frac{\delta\Gamma}{\Gamma}\right), \tag{17}$$
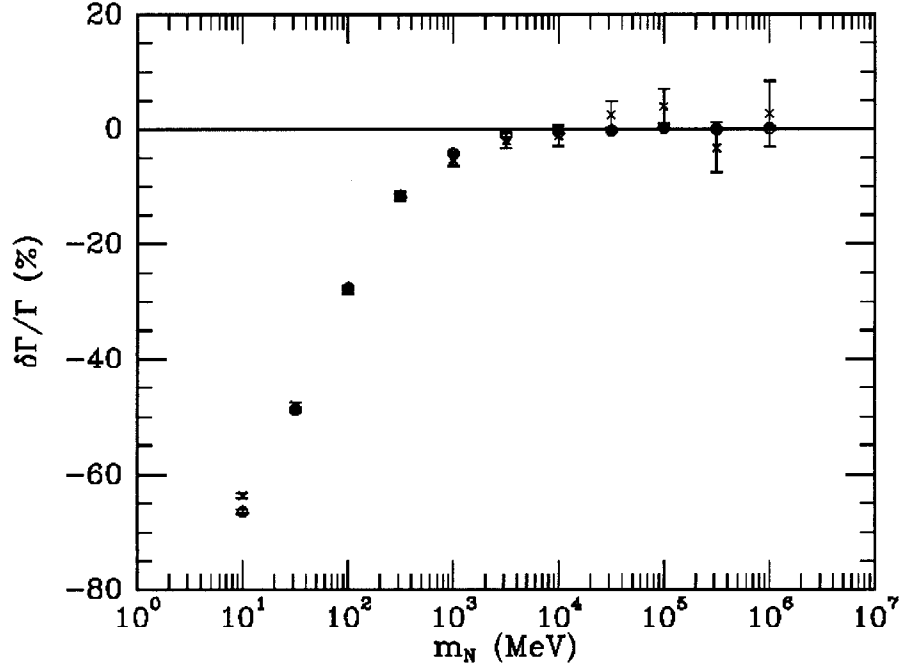
8

Figure 5: Kinematics test for $T = 5.0\,\text{MeV}$ (see text). Circles are the five-dimensional integration and crosses are the three-dimensional integration.

where $\delta\Gamma = \sum_i \delta\Gamma_i, \Gamma = \sum_i \Gamma_i$ and i runs over the three reactions that convert neutrons to protons (or vice versa). A plot of the relative finite-mass rate corrections as a function of temperature is shown in Fig. 7. At the crucial freeze-out epoch ($T \simeq 0.8\,\text{MeV}$), both rates are corrected downward, with $\delta\Gamma_{p\to n}/\Gamma_{p\to n} = -0.43\%$ and $\delta\Gamma_{n\to p}/\Gamma_{n\to p} = -0.55\%$

One subtlety that we have not mentioned is the fact that in the standard code the weak rates are normalized to the measured free-neutron decay rate. This means that free-neutron decay has already been "corrected" for the zero-temperature, finite-nucleon-mass effect. Since the other rates are normalized to τ_n, they too include a piece of the finite-nucleon-mass correction, where the finite-nucleon-mass correction to free-neutron decay is δ_n. To properly implement our results in the standard code we must "remove" this correction, so that Eq. (17) is actually implemented as

$$\Gamma_{p\to n} = \Gamma_{p\to n}^{\text{std}} \left(1 + \frac{\delta\Gamma}{\Gamma}\right)(1 - \delta_n)$$

$$\Gamma_{n\to p} = \Gamma_{n\to p}^{\text{std}} \left(1 + \frac{\delta\Gamma}{\Gamma}\right)(1 - \delta_n). \tag{18}$$

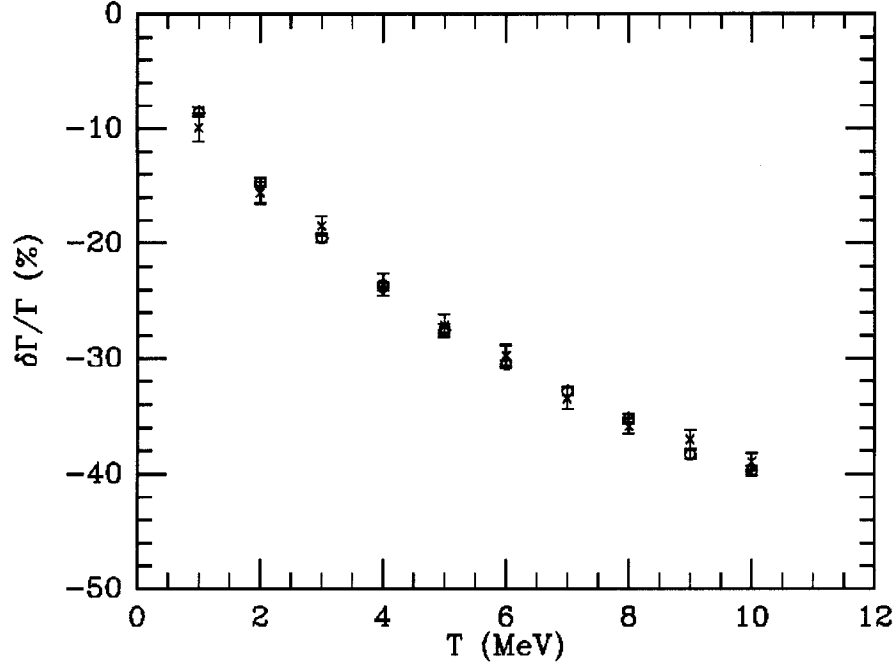To compute δ_n we began with the twelve-dimensional phase-space integral for neutron

9

Figure 6: Kinematics test with $m_N = 100.0$MeV (see text). Circles are the five-dimensional integration and crosses are the three-dimensional integration.

decay,

$$\Gamma_{n \to pe\nu} = \frac{1}{n_p} \int \prod_i d\Pi_i (2\pi)^4 |\mathcal{M}|^2 \delta^{(4)}(e + p - \nu - n) f_n (1 - f_p)(1 - f_e)(1 - f_\nu). \qquad (19)$$

In the zero-temperature limit, $f_n = (n_n/2)(2\pi)^3 \delta^{(3)}(\mathbf{p_n})$, and $(1 - f_p) = (1 - f_e) = (1 - f_\nu) = 1$. This expression can be simplified to the following two-dimensional integral:

$$\Gamma_{n \to pe\nu} = \frac{1}{2^7 \pi^3} \int_{m_e}^{Q - (Q^2 - m_e^2)/2m_N} dE_e \int_{-1}^{1} d\cos\theta_\nu \frac{|\mathcal{M}|^2 p_e E_\nu}{m_n E_p |\mathcal{J}|}, \qquad (20)$$

$$|\mathcal{J}| = 1 + \frac{E_\nu + p_e \cos\theta_\nu}{E_p}, \qquad (21)$$

$$E_p = m_n - E_\nu - E_e, \qquad (22)$$

$$E_\nu = \frac{m_n^2 - m_p^2 + m_e^2 - 2m_n E_e}{2(m_n - E_e + p_e \cos\theta_\nu)}, \qquad (23)$$

where $|\mathcal{J}|$ is the Jacobian introduced due to integration over the energy delta function. Note that the full matrix element is used. Using standard techniques, we integrated this expression and found the zero-temperature neutron decay correction, $\delta_n \equiv \Gamma_{n \to pe\nu} - \Gamma_{n \to pe\nu}^\infty = -0.206\%$.
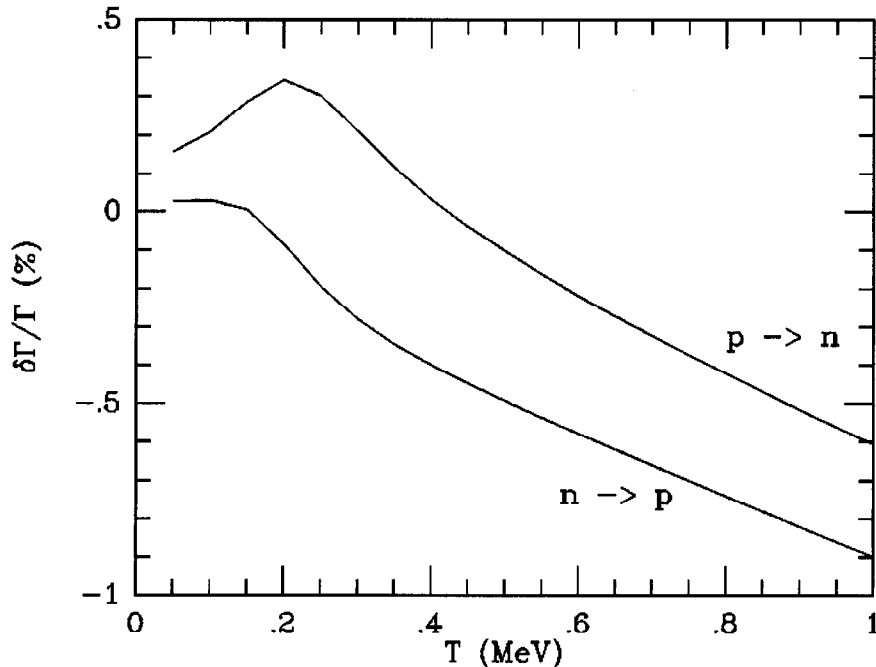
10

Figure 7: Corrections to $\Gamma_{p\to n}(T)$ and $\Gamma_{n\to p}(T)$.

5   Results and Conclusions

Our results, which were obtained for three massless-neutrino species and a mean neutron lifetime of 887 sec [32], are shown in Fig. 8. Plotted are the fractional changes in the mass abundances of D, ^{3}He, ^{4}He and ^{7}Li versus the baryon-to-photon ratio η. The relative change in ^{4}He is approximately 0.47% − 0.50% over a large interval, $10^{-11} \le \eta \le 10^{-8}$. Over the most interesting part of the interval, $\eta = (2 - 7) \times 10^{-10}$, $\Delta Y/Y = (0.49 - 0.50)\%$. Over the full interval in η, the fractional change in the other light elements span the range 0.06% to 2.8%. Unlike ^{4}He, the inferred primordial abundances of these elements are known to nowhere near this accuracy and these changes are of little relevance at present.

Several years ago the effect of finite nucleon mass on the yields of nucleosynthesis was estimated by Gyuk and Turner [33] based on an approximation scheme developed by Seckel [34]. Seckel estimated the lowest-order correction, i.e., terms of order $1/m_N$, to the weak rates and Gyuk and Turner incorporated them into the standard code. Our finite-nucleon-mass corrections are generally consistent with Seckel's estimates for the changes in the rates; however, there are significant qualitative and quantitative differences. Likewise, our calculation of ΔY is consistent, but significantly smaller, than that of Gyuk and Turner who found $\Delta Y \simeq 0.006 Y$ based on Seckel's scheme.
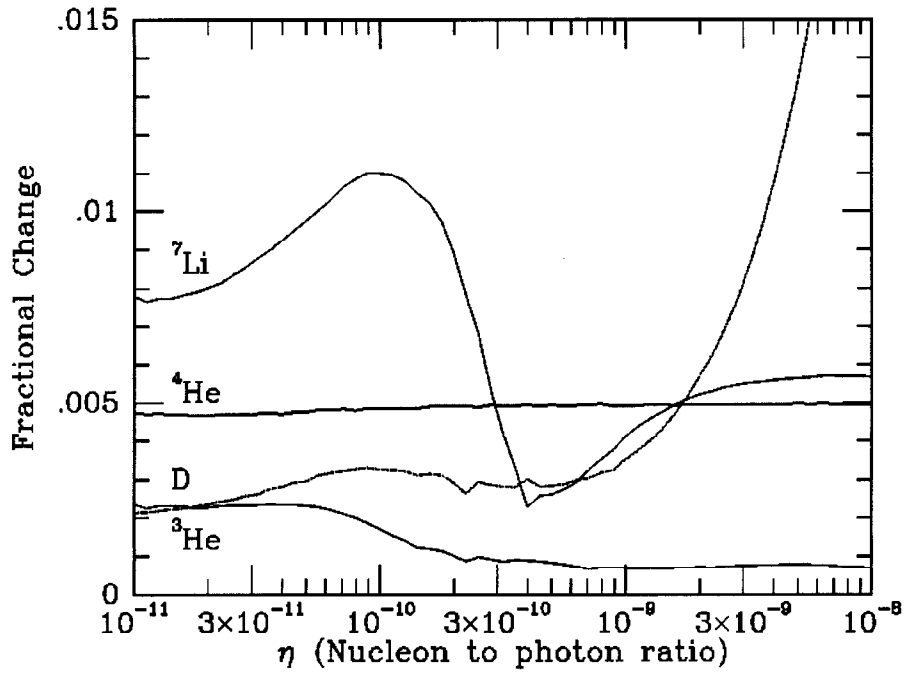
11

Figure 8: Finite-mass corrections to light element abundances. For ^{4}He the fractional change is in the mass fraction; for the others it is in the number relative to H.

Acknowledgements

A   Appendix: The Matrix Element

Here we present the full matrix element to leading order in the weak interaction coupling constant [34, 35]. The particles labeled by 1 and 3 are the incident and outgoing leptons, and by 2 and 4 are the incident and outgoing nucleons. The matrix element is expressed in terms of the relativistic invariants s and t. Here, $s = (1 + 2)^2 = (3 + 4)^2$ and $t = (1 - 3)^2 = (2 - 4)^2$, where $1, 2, 3, 4$ are the four-momenta of the respective particles, $f_2 = 1.81$ is the anomalous weak magnetic moment of the nucleon, and $g_A = 1.257$ is the ratio of axial to vector coupling of the nucleon.

This expression applies to all six weak processes. For anti-leptonic, two-body processes,

e.g., $e^+n \to \bar{\nu}_e p$, $g_A \to -g_A$. For $n \to pe\nu$, $s = (-1+2)^2$ and $t = (-1-3)^2$ and for $pe\nu \to n$, $s = (1+2)^2$ and $t = (1+3)^2$.

$$
\begin{aligned}
|\mathcal{M}|^2 &= G_F^2 \left(t_1 + t_2 + t_3 + t_4 + t_5 + t_6\right), \\
t_1 &= 16 f_2/m_N \times \\
&\quad (-m_1^4 m_4 + m_1^2 m_2^3 - m_1^2 m_2^2 m_4 + m_1^2 m_2 m_3^2 - m_1^2 m_2 s \\
&\quad -m_1^2 m_2 t + m_1^2 m_3^2 m_4 + m_1^2 m_4 s - m_2^3 t + m_2^2 m_4 t \\
&\quad -m_2 m_3^4 - m_2 m_3^2 m_4^2 + m_2 m_3^2 s + m_2 m_4^2 t + m_2 t^2 \\
&\quad +m_3^2 m_4^3 - m_3^2 m_4 s - m_3^2 m_4 t - m_4^3 t + m_4 t^2), \\
t_2 &= 8 \times \\
&\quad (m_1^2 m_2^2 - 2 m_1^2 m_2 m_4 + 2 m_1^2 m_3^2 + m_1^2 m_4^2 - 2 m_1^2 s \\
&\quad -m_1^2 t + m_2^2 m_3^2 + 2 m_2^2 m_4^2 - 2 m_2^2 s - m_2^2 t \\
&\quad -2 m_2 m_3^2 m_4 + 2 m_2 m_4 t + m_3^2 m_4^2 - 2 m_3^2 s - m_3^2 t - 2 m_4^2 s \\
&\quad -m_4^2 t + 2 s^2 + 2 s t + t^2), \\
t_3 &= 4 f_2^2/m_N^2 \times \\
&\quad (m_1^4 m_2^2 - 2 m_1^4 m_2 m_4 - 3 m_1^4 m_4^2 - m_1^4 t + 2 m_1^2 m_2^4 \\
&\quad +2 m_1^2 m_2^2 m_3^2 - 4 m_1^2 m_2^2 s - 3 m_1^2 m_2^2 t + 4 m_1^2 m_2 m_3^2 m_4 - 2 m_1^2 m_2 m_4 t \\
&\quad +2 m_1^2 m_3^2 m_4^2 - 2 m_1^2 m_3^2 t - 2 m_1^2 m_4^4 + 4 m_1^2 m_4^2 s + m_1^2 m_4^2 t \\
&\quad +4 m_1^2 s t + m_1^2 t^2 - 2 m_2^4 m_3^2 - 2 m_2^4 t - 3 m_2^3 m_3^4 \\
&\quad +4 m_2^2 m_3^2 s + m_2^2 m_3^2 t + m m_2^2 s t + 2 m_2^2 t^2 - 2 m_2 m_3^4 m_4 \\
&\quad -2 m_2 m_3^2 m_4 t + 4 m_2 m_4 t^2 + m_3^4 m_4^2 - m_3^4 t + 4 m_3^2 s t \\
&\quad +m_3^2 t^2 - 2 m_4^4 t + 4 m_4^2 s t + 2 m_4^2 t^2 - 4 s^2 t \\
&\quad -4 s t^2), \\
t_4 &= 8 g_A^2 \times \\
&\quad (m_1^2 m_2^2 + 2 m_1^2 m_2 m_4 + 2 m_1^2 m_3^2 + m_1^2 m_4^2 - 2 m_1^2 s \\
&\quad -m_1^2 t + m_2^2 m_3^2 + 2 m_2^2 m_4^2 - 2 m_2^2 s - m_2^2 t \\
&\quad +2 m_2 m_3^2 m_4 - 2 m_2 m_4 t + m_3^2 m_4^2 - 2 m_3^2 s - m_3^2 t \\
&\quad -2 m_4^2 s - m_4^2 t + 2 s^2 + 2 s t + t^2), \\
t_5 &= 16 g_A^2 f_2/m_2 \times \\
&\quad (-m_1^2 m_2^3 - m_1^2 m_2^2 m_4 + m_1^2 m_2 m_4^2 + m_1^2 m_2 t + m_1^2 m_4^3 \\
&\quad +m_1^2 m_4 t + m_2^3 m_3^2 + m_2^3 t + m_2^2 m_3^2 m_4 + m_2^2 m_4 t \\
&\quad -m_2 m_3^2 m_4^2 + m_2 m_3^2 t + m_2 m_4^2 t - 2 m_2 s t - m_2 t^2 \\
&\quad -m_3^2 m_4^3 + m_3^2 m_4 t + m_4^3 t - 2 m_4 s t - m_4 t^2), \\
t_6 &= 16 g_A \times
\end{aligned}
$$

13

$$(-m_1^2 m_2^2 + m_1^2 m_4^2 + m_1^2 t + m_2^2 m_3^2 + m_2^2 t$$
$$-m_3^2 m_4^2 + m_3^2 t + m_4^2 t - 2st - t^2).$$

References

[1] C.J. Copi, M.S. Turner, and D.N. Schramm, Science **267**, 192 (1995).

[2] J. Yang, M.S. Turner, G. Steigman, D.N. Schramm, and K.A. Olive, Astrophys. J. **281**, 493 (1984).

[3] T.P. Walker et al., Astrophys. J. **376**, 51 (1991).

[4] C.J. Copi, M.S. Turner, and D.N. Schramm, Phys. Rev. D **55**, 3309 (1997).

[5] V.F. Schvartsman, JETP Lett. **9**, 154 (1969).

[6] G. Steigman, D.N. Schramm, and J. Gunn, Phys. Lett. B **66**, 202 (1988).

[7] L. Krauss and P. Romanelli, Astrophys. J. **358**, 47 (1990).

[8] M.S. Smith, L.H. Kawano, and R.A. Malaney, Astrophys. J. Suppl. **85**, 219 (1993).

[9] P. Kernan, PhD thesis, Ohio State University, 1993.

[10] D. Dicus et al., Phys. Rev. D **26**, 2694 (1982).

[11] G.J. Matthews, T. Kajino, and M. Orito, Astrophys. J. **456**, 98 (1996).

[12] S. Dodelson and M.S. Turner, Phys. Rev. D **46**, 3372 (1992).

[13] B. Fields, S. Dodelson, and M.S. Turner, Phys. Rev. D **47**, 4309 (1993).

[14] M. Spite and F. Spite, Nature **297**, 483 (1982).

[15] M. Spite, J.P. Maillard, and F. Spite, Astron. Astrophys. **141**, 56 (1984).

[16] R. Rebolo, P. Molaro, and J. Beckman, Astron. Astrophys. **192**, 192 (1988).

[17] L. Hobbs and J. Thorburn, Astrophys. J. **375**, 116 (1991).

[18] K. Olive and D.N. Schramm, Nature **360**, 439 (1992).

[19] J. Thorburn, Astrophys. J. **421**, 318 (1994).

[20] M.H. Pinsonneault, C.P. Deliyannis, and P. Demarque, Astrophys. J. Suppl. **78**, 179 (1992).

[21] M. Lemoine, D.N. Schramm, J. Truran, and C.J. Copi, astro-ph/9610092 (1996).

[22] D.S.P. Dearborn, D.N. Schramm, and G. Steigman, Astrophys. J. **302**, 35 (1986).

[23] G. Steigman and M. Tosi, Astrophys. J. **453**, 173 (1995).

[24] C.J. Copi, D.N. Schramm, and M.S. Turner, Astrophys. J. Lett. **455**, L95 (1995).

[25] B.E.J. Pagel, Physica Scripta **T36**, 7 (1991).

[26] B.E.J. Pagel and A. Kazlauskas, Mon. Not. R. Astron. Soc. **256**, 49 (1992).

[27] K.A. Olive and G. Steigman, Astrophys. J. Suppl. **97**, 49 (1995).

[28] D. Tytler, S. Burles, and D. Kirkman, astro-ph/9612121 , and references therein.

[29] L. Kawano, Fermilab-PUB-92/04-A, 1992.

[30] L. Kawano and D.N. Schramm, Nucl. Instrum. Methods A **284**, 84 (1989).

[31] S. Weinberg, *Gravitation and Cosmology*, (J. Wiley, New York, 1972) pp. 545-548.

[32] R.M. Barnett et al., Phys. Rev. D **54**, 1 (1996).

[33] G. Gyuk and M.S. Turner, astro-ph/9307025 (1993).

[34] D. Seckel, hep-ph/9305311 (1993).

[35] L. Bergstrom, private communication, (1996).